Solar Energy Materials & Solar Cells 102 (2012) 208–211

Contents lists available at SciVerse ScienceDirect

Solar Energy Materials & Solar Cells

journal homepage: www.elsevier.com/locate/solmat

Letter

Fabrication and characterization of n-$In_{0.4}Ga_{0.6}N$/p-Si solar cell

Binh-Tinh Tran [a], Edward-Yi Chang [a,*], Hai-Dang Trinh [a], Ching-Ting Lee [b], Kartika Chandra Sahoo [a], Kung-Liang Lin [a], Man-Chi Huang [a], Hung-Wei Yu [a], Tien-Tung Luong [a], Chen-Chen Chung [a], Chi-Lang Nguyen [a]

[a] Department of Materials Science and Engineering, National Chiao Tung University, 1001 University Road, Hsinchu, Taiwan
[b] Department of Electrical Engineering, National Cheng Kung University, Taiwan

ARTICLE INFO

Article history:
Received 18 December 2011
Received in revised form
21 February 2012
Accepted 26 March 2012
Available online 19 April 2012

Keywords:
MOCVD
InGaN
Si
Solar cell
ITO

ABSTRACT

Electro-optic characteristics of a fabricated n-$In_{0.4}Ga_{0.6}N$/p-Si hetero-structure solar cell on Si substrate with Al and ITO (or Ti/Al/Ni/Au) materials for p and n-type contacts were investigated in this letter. The solar cell devices with ITO as n-type contacts were also compared to the solar cell using Ti/Al/Ni/Au as n-type contact in this study. High short-circuit current density observed for solar cell with ITO as n-type contacts due to the increased amount of light reaching the solar cell. The device with ITO contact exhibited an open-circuit voltage (V_{oc}) of 1.52 V and a short-circuit current density (J_{sc}) of 8.68 mA/cm^2 with 54% fill factor. The conversion and external quantum efficiency (*EQE*) of the solar cell were 7.12 and 20.8%, respectively. Besides, a relationship between V_{oc} and In content in the $In_xGa_{1-x}N$ alloys for this type of solar cell was also derived.

1. Introduction

The $In_xGa_{1-x}N$ alloys attract a lot of attention for optoelectronic applications due to their bandgap range (i.e. continuously from ~0.67 eV to 3.4 eV) and higher theoretical mobility, high saturation velocity, and high absorption rate. This material system is very promising for multijunction solar cell application. The theoretical calculation indicates that $In_xGa_{1-x}N$ alloys with about 40% In content can fulfill the requirements as active material for solar cells with solar energy conversion efficiency greater than 50% [1]. However, to develop this III-nitride material, several major challenges need to be overcome. First, there is a lack of a suitable substrate in terms of lattice and thermal expansion coefficient mismatches for the epitaxial growth of $In_xGa_{1-x}N$ with low dislocation density. Usually, SiC and sapphire are the most common substrates used to grow III-nitride materials, but with high dislocation density in the range of $\sim 10^7$ to 10^{10} cm^{-2} [2,3]. Second, the large lattice mismatch between InN and GaN usually leads to a miscibility gap, which can cause phase separation [4], V-pit defects, and InN segregation [5,6]. Therefore, it is difficult to grow high indium content $In_xGa_{1-x}N$ films with good quality, which have great potential for solar cell applications, on these substrates. There are only a few reports on $In_xGa_{1-x}N$ films grown on Si substrate with In content below 40% and no reports so far on fabrication of $In_xGa_{1-x}N$ on Si substrate with high In content ($x > 40\%$) for solar cell application. In this letter, we report on the fabrication and characterization of a n-$In_{0.4}Ga_{0.6}N$/p-Si hetero-structure solar cell. We also compare the characteristics of the solar cell fabricated using two different n-type contact materials. The detailed development process for the n-$In_{0.4}Ga_{0.6}N$/p-Si hetero-structure has been previously reported in [7].

2. Experimental procedures

The growth of $In_{0.4}Ga_{0.6}N$ film on GaN/AlN/Si(111) substrate was carried out using a Metal Organic Chemical Vapor Deposition (MOCVD) in an EMCORE Model D-180 rotating disk vertical reactor and the detailed growth process has been reported as mentioned above. In brief, the growth process consists of a 50 nm AlN buffer grown on Si substrate at 1010 °C followed by a 0.6-μm-thick GaN film deposition at 1030 °C. Finally, a 300-nm-thick $In_{0.4}Ga_{0.6}N$ film was grown epitaxially on top of the GaN film at 740 °C with the growth pressure of 300 Torr. Then we checked the material quality of the n-$In_{0.4}Ga_{0.6}N$/p-Si hetero-structure by doing a photoluminescence measurement (PL) on 3 different positions on the wafer surface before the fabrication of the solar cell. The fabricated solar cells had a cell area of 1×1 cm^2. The radius pattern for n-type electrode on each cell was 0.33 mm and was fabricated by direct deposition of Ti/Al/Ni/Au (200/1200/250/1000 Å) on the top of the $In_{0.4}Ga_{0.6}N$ film by electron beam

* Corresponding author. Tel.: +886 3 5131536.
E-mail address: edc@mail.nctu.edu.tw (E.-Y. Chang).

0927-0248/$ - see front matter © 2012 Elsevier B.V. All rights reserved.
http://dx.doi.org/10.1016/j.solmat.2012.03.030

evaporation (device-A). The p-type contact was formed by evaporation of 1000-Å-thick Al on the backside of p-Si substrate. For device-B a 2000 Å thick ITO layer was used as n-type contact while keeping all other structures the same as in device-A. The $In_{0.4}Ga_{0.6}N$ film was intrinsically n-type due to the donor-like nature of the native defects of the material and the Si substrate was boron doped p-type substrate with sheet resistance of 5–10 Ω cm. The electron concentration was in the order of 10^{19} cm^{-3} as obtained from the Hall measurements. We presented the fabrication process of device-B in Fig. 1, and device-A is similar to that of device-B. The current–voltage characteristics of the devices were measured under AM 1.5G illumination (one sun, air mass 1.5 global spectrum).

3. Results and discussion

The PL measurements of the $In_{0.4}Ga_{0.6}N$ film were conducted at room temperature (RT) with an incident wavelength of 325 nm and the measured spectral peaks at 3 different positions of the wafer are presented in Fig. 2. The main PL peak shows good results across the wafer and the weak peaks beside the main peak in Fig. 2 correspond to Fabry–Perot interferences between the GaN/Si interface and the surface [8]. These weak PL peaks are related to the phase separation of $In_xGa_{1-x}N$ due to the weak bonding between In–N and Ga–N. However, this result is in good agreement with the reports of $In_xGa_{1-x}N$ grown on other substrates [9–12].

To investigate the device characteristics, the dark current of the n-$In_{0.4}Ga_{0.6}N$/p-Si hetero-structure solar cells were measured and presented in Fig. 3. The leakage current of device-A (used Ti/Al/Ni/Au as n-type contact) was higher than device-B (used ITO as n-type contact) and the values of the leakage current were 3.7×10^{-6} and 0.48×10^{-7} A under a bias of −7 V for device-A and device-B, respectively. This result indicates that the n-$In_{0.4}Ga_{0.6}N$/p-Si hetero-structure solar cell using ITO as n-type contact is better than Ti/Al/Ni/Au. Fig. 4 shows the current density versus the voltage characteristics of the devices under AM 1.5G. The measured V_{oc} and J_{sc} for device-B were 1.52 V and 8.68 mA/cm^2, respectively. It can be observed that the V_{oc} and J_{sc} of device-B

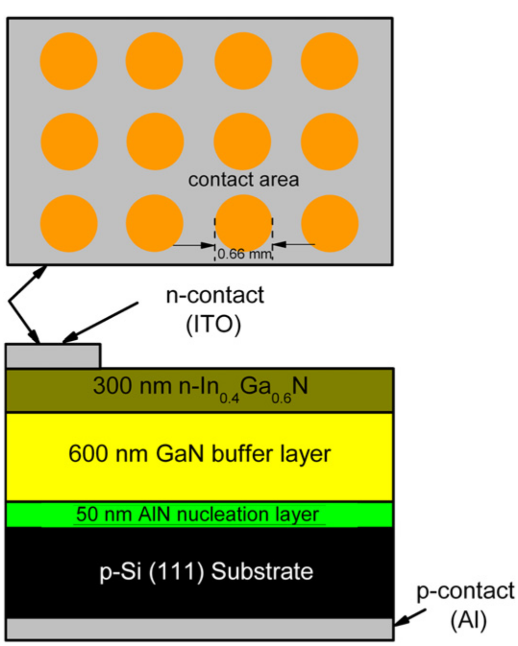

Fig. 1. Solar cell structure with Al and ITO materials for p and n-type contacts (device-B), respectively.

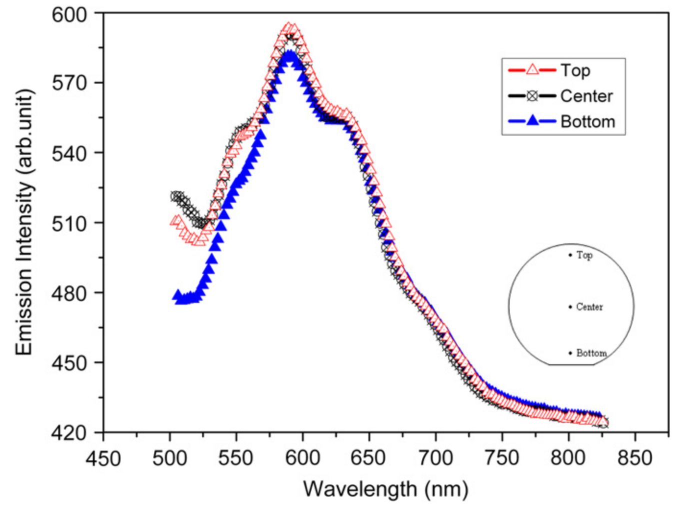

Fig. 2. Photoluminescence spectra of the samples measured at 3 different positions on the wafer conducted at room temperature.

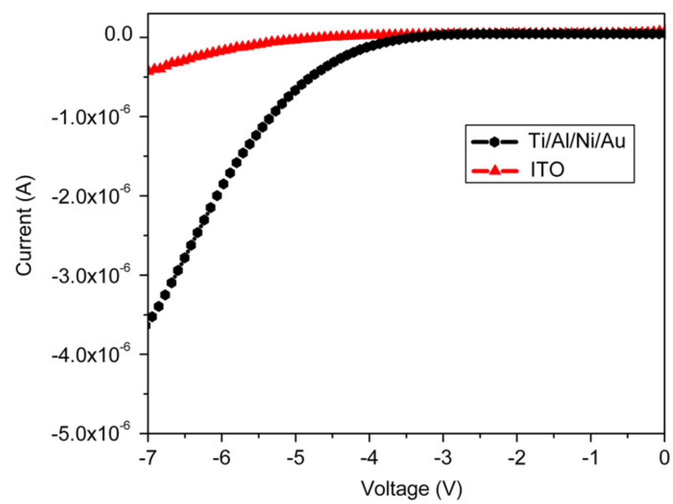

Fig. 3. Dark current–voltage curves for the n-$In_{0.4}Ga_{0.6}N$/p-Si solar cell.

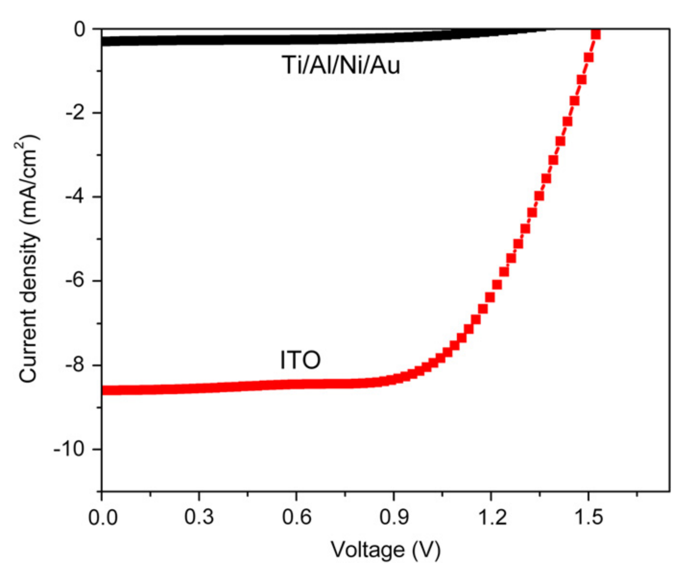

Fig. 4. Typical current–voltage characteristics of the n-$In_{0.4}Ga_{0.6}N$/p-Si solar cell with Ti/Al/Ni/Au and ITO contact materials.

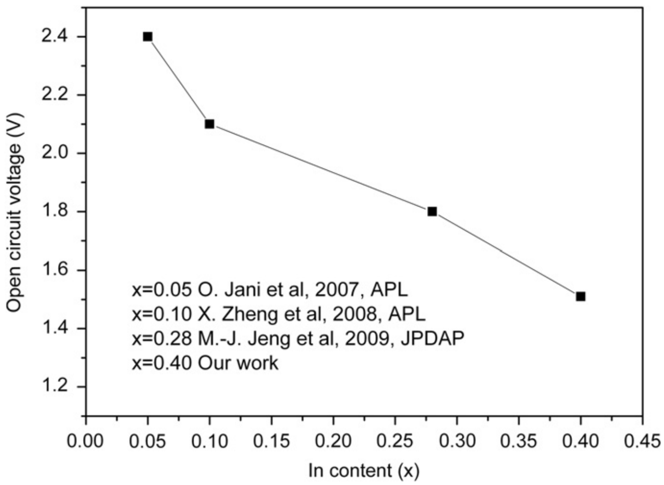

Fig. 5. Open-circuit voltage as a function of In content plotted with other reported data.

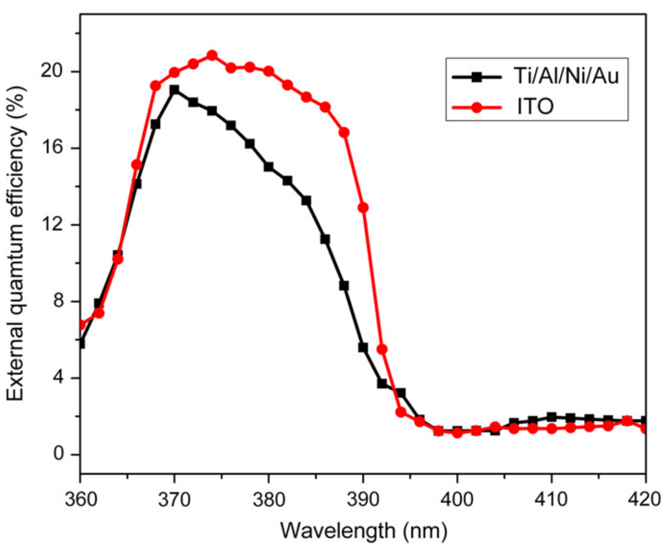

Fig. 6. External quantum efficiency for the n-$In_{0.4}Ga_{0.6}N$/p-Si solar cell with different types of contact materials.

were larger than those of device-A due to its transparent contact (ITO), which is attributed to more light hitting the device and the improvement in the leakage current. For device-A, we can easily observe that the cell only slightly responds to the white light because it only responds to ultraviolet light [13,14] and this phenomenon needs further investigation. The fill factor and conversion efficiency of the n-$In_{0.4}Ga_{0.6}N$/p-Si hetero-structure solar cell were calculated using the measured current density and voltage curves from Fig. 4. The calculated fill factor and conversion efficiency for device-B were 54 and 7.12%, respectively. However, the V_{oc} of device-B was still smaller as compared to other reports [14–16]. From this comparison, it can be found that the V_{oc} value decreases with the increase of In content. This decrease in V_{oc} could be due to either the degradation of electro-optic or material properties or both. This can be explained using the equation written below [16]

$$V_{OC} = \frac{E_g}{q} + \left(\frac{nkT}{q}\right)\ln(J_{sc}) - \left(\frac{nkT}{q}\right)\ln(J_{00}) \quad (1)$$

where E_g is the energy bandgap, KT/q the thermal voltage, n the ideality factor, J_{sc} the short-circuit current density and J_{00} a weak temperature dependent pre-factor. From this equation, the third term is related to the quality of material, and the second term, in contrast to the first term, changes very little when the indium content changes and V_{oc} decreases linearly with E_g based on the Eq. (1). However, the experimental results show not fully linear as plotted in Fig. 5. The problem can be attributed to the defects in materials. The three-first square points 1, 2 and 3 in Fig. 5 are taken from Refs. [14–16] and the last one is our data measured from n-$In_{0.4}Ga_{0.6}N$/p-Si hetero-structure solar cell (device-B). From the data, it is clear that the V_{oc} for hetero-structure device still decreases with the increase of In content though there is a small deviation. The results with different In contents samples follow the same variation and clearly indicate that In content plays an important role in determining V_{oc} for the $In_xGa_{1-x}N$ solar cell.

Fig. 6 shows the *EQE* for the device-A and device-B. We used Acton monochrometer to disperse Xe lamp for this measurement under AM 1.5G condition at RT, and a calibrated silicon photodetector was used to detect the incident light power. The *EQE* was estimated from the ratio between the number of incident photons and the number of measured electrons. This figure shows the quantum efficiency as a function of excitation wavelength. The results demonstrate that device-A and device-B deliver an external quantum efficiency of about 19.0% and 20.8%, respectively. Device-B shows an improved external quantum efficiency as compared to device-A and both device structures show comparable performances as compared with complicated structure reported previously [17].

4. Conclusions

In summary, we report the fabrication of n-$In_{0.4}Ga_{0.6}N$/p-Si solar cell on Si substrate for the first time. We investigated ITO and Ti/Al/Ni/Au as n-type contact and found that the device with ITO as n-type contact demonstrated an enhanced short-circuit current density due to the increased amount of light that was absorbed by the solar cell as compared to the device using Ti/Al/Ni/Au as n-type contact. The device with ITO contact showed good photovoltaic performances and clear spectral response with a fill factor of about 54%, an external quantum efficiency of 20.8 and 14% at 375 and 390 nm, respectively, and the overall conversion efficiency of 7.12%. This is the highest conversion efficiency reported for an $In_xGa_{1-x}N$ based solar cell. Overall, the study demonstrates the potential of using $In_xGa_{1-x}N$ for high efficiency solar cell applications.

Acknowledgment

The authors would like to thank the Taiwan National Science Council (under research grant nos. NSC98-2923-E-009-002-MY3 and NSC99-2221-E-009-170-MY3) for providing the financial support.

References

[1] A.D. Vos, Endoreversible Thermodynamics of Solar Energy Conversion, Oxford University Press, Oxford, 1992, pp. 90.
[2] N. Faleev, H. Lu, W.J. Schaff, Low density of threading dislocations in AlN grown on sapphire, Journal of Applied Physics 101 (2007) 093516-1–093516-3.
[3] N. Faleev, C. Honsberg, O. Jani, I. Ferguson, Crystalline perfection of GaN and AlN epitaxial layers and the main features of structural transformation of crystalline defects, Journal of Crystal Growth 300 (2007) 246–250.
[4] A. Wakahara, T. Tokuda, X.Z. Dang, S. Noda, A. Sasaki, Compositional inhomogeneity and immiscibility of a GaInN ternary alloy, Applied Physics Letters 71 (1997) 906–908.
[5] I.-H. Kim, H.-S. Park, Y.-J. Park, T. Kim, Formation of V-shaped pits in InGaN/GaN multiquantum wells and bulk InGaN films, Applied Physics Letters 73 (1998) 1634–1636.

[6] R. Singh, D. Doppalapudi, T.D. Moustakas, L.T. Romano, Phase separation in InGaN thick films and formation of InGaN/GaN double heterostructures in the entire alloy composition, Applied Physics Letters 70 (1997) 1089–1091.
[7] B.-T. Tran, E.-Y. Chang, K.-L. Lin, Y.-Y. Wong, K.C. Sahoo, H.-Y. Lin, M.-C. Huang, H.-Q. Nguyen, C.-T. Lee, H.-D. Trinh, Growth of high-quality $In_{0.4}Ga_{0.6}N$ film on Si substrate by metal organic chemical vapor deposition, Applied Physics Express 4 (2011) 115501-1–115501-3.
[8] A. Kraus, S. Hammadi, J. Hisek, R. Buß, H. Jönen, H. Bremers, U. Rossow, E. Sakalauskas, R. Goldhahn, A. Hangleiter, Growth and characterization of InGaN by RF-MBE, Journal of Crystal Growth 323 (2011) 72–75.
[9] R. Dahal, B. Pantha, J. Li, J.Y. Lin, H.X. Jiang, InGaN/GaN multiple quantum well solar cells with long operating wavelengths, Applied Physics Letters 94 (2009) 063503–063505.
[10] I. Gherasoiu, K.M. Yu, L.A. Reichertz, V.M. Kao, M. Hawkridge, J.W. Ager, W. Walukiewicz, High quality $In_xGa_{1-x}N$ thin films with $x>0.2$ grown on silicon, Physica Status Solidi B 247 (2010) 1747–1749.
[11] I.W. Feng, X.K. Cao, J. Li, J.Y. Lin, H.X. Jiang, N. Sawaki, Y. Honda, T. Tanikawa, J.M. Zavada, Photonic properties of erbium doped InGaN alloys grown on Si (001) substrates, Applied Physics Letters 98 (2011) 081102-1–081102-3.
[12] M. Gartner, C. Kruse, M. Modreanu, A. Tausendfreund, C. Roder, D. Hommel, Optical characterization of $In_xGa_{1-x}N$ alloys, Applied Surface Science 253 (2006) 254–257.
[13] O. Jani, C. Honsberg, A. Asghar, D. Nicol, I. Ferguson, A. Doolittle, S. Kurtz, Characterization and Analysis of InGaN Photovoltaic Devices, Presented at the Photovoltaic Specialists Conference, Conference Record of the Thirty-first IEEE, 2005.
[14] O. Jani, I. Ferguson, C. Honsberg, S. Kurtz, Design and characterization of GaN/InGaN solar cells, Applied Physics Letters 91 (2007) 132117-1–132117-3.
[15] X. Zheng, R.-H. Horng, D.-S. Wuu, M.-T. Chu, W.-Y. Liao, M.-H. Wu, R.-M. Lin, Y.-C. Lu, High-quality InGaN/GaN heterojunctions and their photovoltaic effects, Applied Physics Letters 93 (2008) 261108-1–261108-3.
[16] J. Ming-Jer, L. Yu-Lin, C. Liann-Be, Temperature dependences of $In_xGa_{1-x}N$ multiple quantum well solar cells, Journal of Physics D: Applied Physics 42 (2009) 105101-1–105101-6.
[17] I.M. Pryce, D.D. Koleske, A.J. Fischer, H.A. Atwater, Plasmonic nanoparticle enhanced photocurrent in GaN/InGaN/GaN quantum well solar cells, Applied Physics Letters 96 (2010) 153501–153503.